

Probing triple Higgs couplings of the Two Higgs Doublet Model at Linear Collider

Abdesslam Arhrib^{1,2}, Rachid Benbrik³, Cheng-Wei Chiang^{1,4}

¹ *Department of Physics and Center for Mathematics and Theoretical Physics,
National Central University, Chungli, Taiwan 320, R.O.C.*

² *Département de Mathématiques, Faculté des
Sciences et Techniques B.P. 416 Tanger, Morocco.*

³ *Department of Physics, Chung Yuan Christian
University, Chungli, Taiwan 320, R.O.C. and*

⁴ *Institute of Physics, Academia Sinica, Taipei, Taiwan 115, R.O.C.*

Abstract

We study double Higgs production at the future Linear Collider in the framework of the Two Higgs Doublet Models through the following channels: $e^+e^- \rightarrow \Phi_i\Phi_j Z$, $\Phi_i = h^0, H^0, A^0, H^\pm$. All these processes are sensitive to triple Higgs couplings. Hence observations of them provide information on the triple Higgs couplings that help reconstructing the scalar potential. We also discuss the double Higgs-strahlung $e^+e^- \rightarrow h^0h^0Z$ in the decoupling limit where h^0 mimics the SM Higgs boson. The processes $e^+e^- \rightarrow h^0h^0Z$ and $e^+e^- \rightarrow h^0H^0Z$ are also discussed in the fermiophobic limit where distinctive signatures such as $4\gamma + X$, $2\gamma + X$ and $6\gamma + X$ are expected in the Type-I Two Higgs Doublet Model.

PACS numbers: 12.60.-t, 13.66.Fg, 13.85.Lg

I. INTRODUCTION

In order to establish the Higgs mechanism for the electroweak symmetry breaking [1], we need to measure the Higgs couplings to fermions and to gauge boson as well as the self-interaction of Higgs bosons. Such measurements, if precise enough, can be helpful in discriminating between models through their sensitivity to quantum corrections, particularly in specific scenarios such as the decoupling limit where Higgs couplings mimic the SM ones.

If electroweak symmetry breaking is achieved by the Higgs mechanism, it is possible to discover at least one light Higgs boson at the Large Hadron Collider (LHC). Such a Higgs boson can be a Standard Model (SM) one or one of those predicted by various extensions of the SM, such as the Minimal Supersymmetric Standard Model (MSSM) or Two Higgs Doublet Model (2HDM).

In case of a discovery of the Higgs boson at the LHC, it may be possible to measure its couplings to gauge bosons and fermions at a certain precision [2]. It has been demonstrated in Ref. [3] that physics at the LHC and the e^+e^- International Linear Collider (ILC) will be complementary to each other in many respects. In many cases, the ILC can significantly improve the LHC measurements.

In recent years there has been growing interest in the study of extended Higgs sectors with more than one Higgs doublet [4, 5, 6]. The simplest extension is the 2HDM; and such a structure is required for the MSSM. Models with two (or more) Higgs doublets predict the existence of charged Higgs bosons. Therefore, the discovery of them would be the conclusive evidence of an extended Higgs sector.

For the linear collider, there have been several studies dedicated to triple Higgs couplings both in the SM and beyond (for a review, see Ref [7]). In Refs. [8] and [9], the double Higgs-strahlung processes and WW fusion both in the SM and MSSM have been addressed. In both cases, the sizes of double Higgs-strahlung processes and WW fusion cross section are rather small. It has been shown in Ref. [10] that for the process of $e^+e^- \rightarrow ZHH$ with $H \rightarrow b\bar{b}$ in the SM, the irreducible background from electroweak and QCD processes can be suppressed down to manageable levels by using kinematics cuts.

At the LHC, the double Higgs production has been studied in Ref. [11] with the conclusion that triple Higgs couplings in the SM and MSSM can be measured provided the background can be rejected sufficiently well.

In 2HDM's, triple and quartic Higgs couplings have been studied for a linear collider in Refs. [12, 13, 14]. In Ref. [12], the triple and quartic couplings have been studied in 2HDM without CP violation. The analytic expressions of triple and quartic couplings are given, but numerical evaluations for the cross section of double Higgs-strahlung are given in the framework of MSSM. Ref. [13] studies the triple Higgs couplings in the framework of 2HDM with CP violation in the Higgs sector. Besides, the numerical analysis for triple Higgs couplings has been presented in MSSM with explicit CP violation.

Ref. [14] concentrates exclusively on the triple Higgs production of the 2HDM at the linear collider, and the cross sections are found to be large. In this paper, we study the double Higgs-strahlung production $e^+e^- \rightarrow \Phi_i\Phi_j Z$, $\Phi_i = h^0, H^0, A^0, H^\pm$ in the general 2HDM, as measurements of these processes can shed some light on the 2HDM triple Higgs couplings. In addition, we also take into account the perturbativity as well as vacuum stability constraints on various parameters in the Higgs potential. We will show that after imposing those constraints, there are still large enough cross sections, a few hundred femtobarns (fb) in some cases, to allow a determination of the 2HDM triple Higgs couplings. We will also study some of these processes in the decoupling limit and in the fermiophobic limit of the so-called type-I 2HDM.

The paper is organized as follows. In the next section, we give a short review of 2HDM as well as a rough numerical estimate of the triple Higgs couplings. In Section III, we evaluate the double Higgs-strahlung production $e^+e^- \rightarrow \Phi_i\Phi_j Z$ in the 2HDM paying special attention to $e^+e^- \rightarrow h^0 h^0 Z$ in the decoupling limit, where h^0 mimics the SM Higgs boson, as well as in the fermiophobic limit. Our findings are summarized in Section IV.

II. SHORT REVIEW OF 2HDM AND TRIPLE HIGGS COUPLINGS

A. Short review of 2HDM

In this section we define the scalar potential to be studied in this article. It has been shown in Refs. [4, 6] that the most general 2HDM scalar potential that is both $SU(2)_L \otimes U(1)_Y$ and CP invariant is given by:

$$V(\Phi_1, \Phi_2) = m_1^2 \Phi_1^\dagger \Phi_1 + m_2^2 \Phi_2^\dagger \Phi_2 - (m_{12}^2 \Phi_1^\dagger \Phi_2 + \text{h.c.}) + \frac{1}{2} \lambda_1 (\Phi_1^\dagger \Phi_1)^2 + \frac{1}{2} \lambda_2 (\Phi_2^\dagger \Phi_2)^2$$

$$+ \lambda_3(\Phi_1^\dagger\Phi_1)(\Phi_2^\dagger\Phi_2) + \lambda_4(\Phi_1^\dagger\Phi_2)(\Phi_1^\dagger\Phi_2) + \frac{1}{2}\lambda_5[(\Phi_1^\dagger\Phi_2)^2 + \text{h.c.}] , \quad (1)$$

where Φ_1 and Φ_2 have weak hypercharge $Y = 1$ and vacuum expectation values (VEV's) v_1 and v_2 , respectively, and λ_i and m_{12} are real-valued parameters. Note that this potential violates the discrete symmetry $\Phi_i \rightarrow -\Phi_i$ softly by the dimension-two term $m_{12}^2(\Phi_1^\dagger\Phi_2)$, and has the same general structure as the scalar potential in the MSSM.

After the electroweak symmetry breaking, the W^\pm and Z gauge bosons acquire their masses. Explicitly, three of the eight degrees of freedom in the two Higgs doublets correspond to the three Goldstone bosons (G^\pm, G^0) and the remaining five become physical Higgs bosons: h^0, H^0 (CP-even), A^0 (CP-odd), and H^\pm with masses $m_{h^0}, m_{H^0}, m_{A^0}$, and m_{H^\pm} , respectively.

The potential in Eq. (1) has ten parameters (including v_1 and v_2). The parameters m_1 and m_2 are fixed by the minimization conditions. The combination $v^2 = v_1^2 + v_2^2$ is fixed as usual by the electroweak breaking scale through $v^2 = (2\sqrt{2}G_F)^{-1}$. We are thus left with seven independent parameters; namely $(\lambda_i)_{i=1,\dots,5}$, m_{12} , and $\tan\beta \equiv v_2/v_1$. Equivalently, we can take instead

$$m_{h^0} , \quad m_{H^0} , \quad m_{A^0} , \quad m_{H^\pm} , \quad \tan\beta , \quad \alpha \quad \text{and} \quad m_{12}. \quad (2)$$

as the seven independent parameters. The angle β diagonalizes both the CP-odd and charged scalar squared-mass matrices and α diagonalizes the CP-even squared-mass matrix. One can easily calculate the physical scalar masses and mixing angles from Eq. (1) in terms of λ_i , m_{12} and v_i , and invert them to obtain λ_i in terms of physical scalar masses, $\tan\beta$, α , and m_{12} [15, 16].

It is straightforward to derive the triple Higgs couplings from the above scalar potential in Eq. (1). In the next section, we list the trilinear scalar self-couplings relevant for our study. Other relevant couplings involving Higgs boson interactions with gauge bosons and fermions can be found in Refs. [4, 17]. We note that Ref. [18] lists the complete Higgs trilinear and quartic interactions for two types of 6-parameter potentials, referred to as 'Potential A' and 'Potential B'. Potential A is equivalent to our potential if $m_{12} \rightarrow 0$, and in this limit the Feynman rules in the next section are in agreement with those in Ref. [18].

There exist three classes of 2HDM's. The main difference among them is in the ways they couple the Higgs fields to matter fields. Assuming natural flavor conservation [19], the two

most popular models are type-I and type-II, denoted by 2HDM-I and 2HDM-II, respectively. In 2HDM-I, the quarks and leptons couple only to one of the two Higgs doublet exactly the same as in the SM. In 2HDM-II, one of the two Higgs fields couples only to down-type quarks (and charged leptons) and the other one only couples to up-type quarks (and neutral leptons) in order to avoid the problem of large flavor-changing neutral currents (FCNC's). This is also the pattern found in the MSSM. The third class of models is type-III, denoted by 2HDM-III. However, they are generally regarded as problematic as FCNC's appear at the tree level [20]. We note that 2HDM-I can lead to a fermiophobic Higgs boson h^0 in the limit where $\cos \alpha = 0$ [4, 21], and the dominant decay mode for the lightest Higgs boson in this model is $h^0 \rightarrow \gamma\gamma$ or $h^0 \rightarrow WW$, depending on its mass. In comparison, 2HDM-II does not have such a feature.

In our analysis we also take into account the following constraints when the independent parameters are varied.

- The extra contributions to the $\Delta\rho$ parameter from the Higgs scalars [22] should not exceed the current limit from precision measurements [23]: $|\Delta\rho| \lesssim 10^{-3}$. Such an extra contribution to $\delta\rho$ vanishes in the limit $m_{H^\pm} = m_{A^0}$. To ensure that $\Delta\rho$ be within the allowed range, we demand only a small splitting between m_{H^\pm} and m_{A^0} .
- From the requirement of perturbativity for the top and bottom Yukawa couplings [24], $\tan\beta$ is constrained to lie in the range $0.3 \leq \tan\beta \leq 100$.
- We note in passing that it has been shown in Ref. [25] that the latest $B \rightarrow X_s\gamma$ branching ratio among others puts a lower bound on the charged Higgs mass, $m_{H^\pm} \gtrsim 250$ GeV, in 2HDM-II. However, the conclusion does not apply to 2HDM-I. Since our analysis is generally valid for both 2HDM-I and 2HDM-II, we still consider values of m_{H^\pm} below 250 GeV for that matter.
- To constrain the scalar-sector parameters we will use both perturbativity constraints on λ_i [26, 27] as well as vacuum stability conditions [28, 29]. We require that all quartic couplings of the scalar potential in Eq. (1) remain perturbative: $\lambda_i \leq 8\pi$ for all i . These perturbative constraints are slightly less constraining than the full set of unitarity constraints [26, 27] established using the high energy approximation and the

equivalence theorem. For vacuum stability conditions, we use [28, 29]:

$$\begin{aligned} \lambda_1 > 0, \quad \lambda_2 > 0, \\ \sqrt{\lambda_1 \lambda_2} + \lambda_3 + \min(0, \lambda_4 - |\lambda_5|) > 0 \end{aligned} \quad (3)$$

- From the experimental point of view, the combined null searches from all four CERN LEP Collaborations give the lower limit $m_{H^\pm} \geq 78$ GeV at 95% confidence level (CL), a limit which applies to all models satisfying $\text{BR}(H^\pm \rightarrow \tau\nu_\tau) + \text{BR}(H^\pm \rightarrow cs)=1$ [30]. Two LEP Collaborations (OPAL and DELPHI) have performed a search for a charged Higgs decaying to AW^* (assuming $m_{A^0} > 2m_b$) and derived limits on the charged Higgs mass [30] comparable to those obtained from the search for $H^\pm \rightarrow cs, \tau\nu$.

For the neutral Higgs bosons, the OPAL and DELPHI Collaborations have put a limit on the masses of h^0 and A^0 in the 2HDM [31, 32]. OPAL concludes that the regions $1 \lesssim m_{h^0} \lesssim 55$ GeV and $3 \lesssim m_{A^0} \lesssim 63$ GeV are excluded at 95% CL, independent of α and $\tan\beta$ [31]. DELPHI Collaboration studies the Higgs to Higgs decay $h^0 \rightarrow A^0 A^0$ in $e^+e^- \rightarrow h^0 Z$ and $h^0 A^0$ production and a large portion of the m_{h^0} - m_{A^0} plane is excluded, depending on the suppression factor that enters the cross section formulas [32]. In what follows, we will assume that all Higgs masses are greater than 100 GeV except in the fermiophobic limit where m_{h^0} can be as light as 60 GeV.

In Fig. 1, we show the allowed region in the m_{12} - $\tan\beta$ plane, taking into account the theoretical constraints mentioned above as well as $\Delta\rho$. The surviving parameter region is quite restricted on the $\tan\beta$ - m_{12} plane. The perturbativity and vacuum stability constraints together dramatically reduce the allowed parameter space of the model. In particular, the perturbativity constraint excludes large values of $\tan\beta$. In fact, with $\sin\alpha = 0.6$, $m_{h^0} = 120$ GeV and for $m_{H^0} = 240$ GeV to 480 GeV, the upper bound on $\tan\beta$ decreases from 10 to 5.4 at $m_{12} = 0$. Nevertheless, for specific values of $m_{12} \neq 0$ and m_H , one can see that values of $\tan\beta$ as large as 70 can still survive the perturbativity and vacuum stability constraints.

However, in the fermiophobic limit of 2HDM-I (right panel of Fig. 1) where $\alpha = \pi/2$, $m_{h^0} = 60$ GeV and $200 \text{ GeV} \leq m_{H^0} \leq 500 \text{ GeV}$, $\tan\beta$ can be as large as about 30 for $m_{12} < 15$ GeV. Note that both plots in Fig. 1 are symmetric under $m_{12} \rightarrow -m_{12}$. For subsequent analyses, we will take $\tan\beta = 10$ as a typical value.

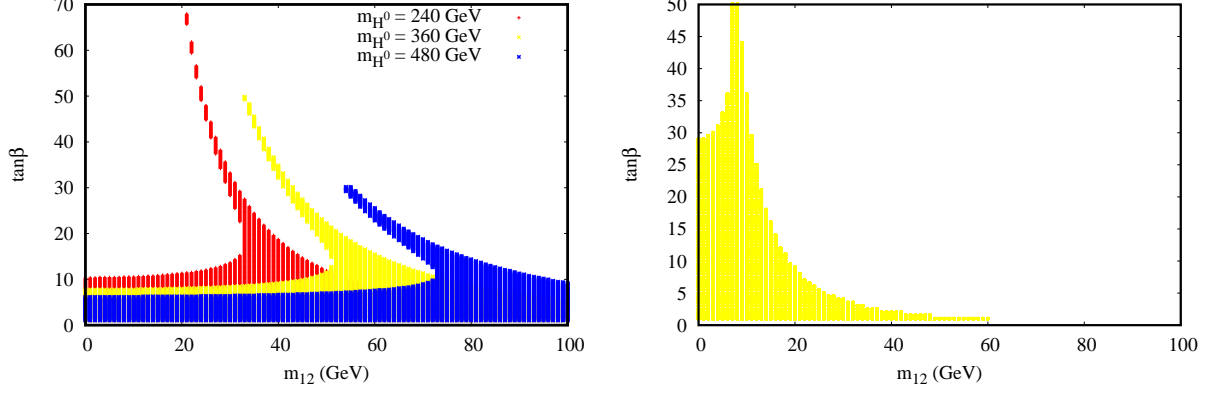


FIG. 1: Allowed region on the m_{12} - $\tan\beta$ plane, taking into account perturbativity and vacuum stability constraints. The common parameters are $m_{H^\pm} = 250$ GeV and $m_{A^0} = 150$ GeV. The left panel uses $(\sin\alpha, m_{h^0}) = (0.6, 120$ GeV) for different values of m_{H^0} , and the right panel is for 200 GeV $\leq m_{H^0} \leq 500$ GeV and $(\sin\alpha, m_{h^0}) = (1, 60$ GeV)

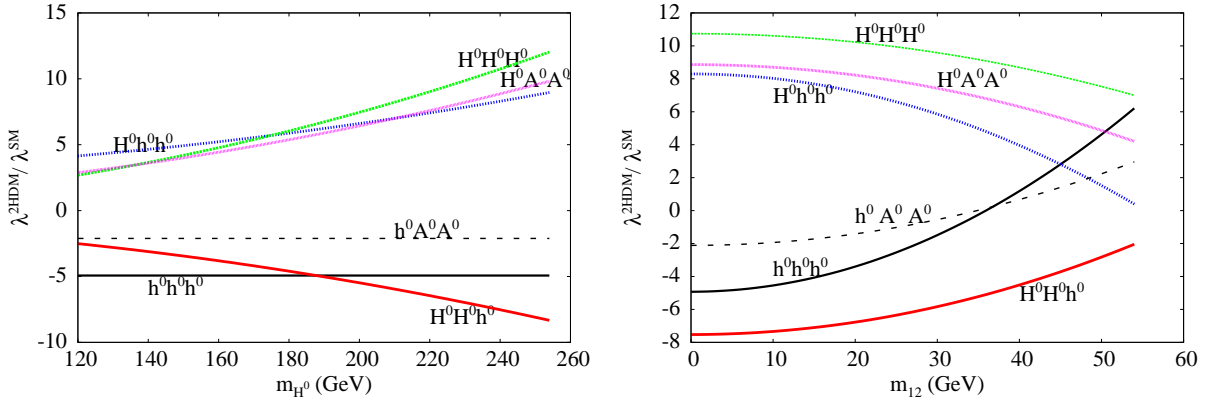


FIG. 2: The 2HDM tree level self couplings $\lambda_{h_i h_j h_k}^{2HDM}$ normalized to the SM self coupling λ_{hhh}^{SM} : (left) as a function of m_{H^0} with $m_{12} = 0$ GeV, (right) and as a function of m_{12} with $m_{H^0} = 240$ GeV. The others parameters are $m_{h^0} = 120$ GeV, $m_{H^\pm} = 140$ GeV, $m_{A^0} = 150$ GeV, $\tan\beta = 10$ and $\sin\alpha = 0.8$

B. Triple Higgs couplings in 2HDM

In this section, we will study the behavior of triple Higgs couplings as a function of the 2HDM parameters m_{h^0} , m_{H^0} , m_{A^0} , m_{H^\pm} , $\tan\beta$, α and m_{12} . These couplings are given by:

$$\lambda_{h^0 h^0 h^0}^{SM} = \frac{-3em_{h^0}^2}{2m_W s_W} \quad (4)$$

$$\lambda_{h^0 h^0 h^0}^{2HDM} = \frac{-3e}{m_W s_W s_{2\beta}^2} \left[(c_\beta c_\alpha^3 - s_\beta s_\alpha^3) s_{2\beta} m_{h^0}^2 - c_{\beta-\alpha}^2 c_{\beta+\alpha} m_{12}^2 \right] \quad (5)$$

$$\lambda_{H^0 H^0 H^0}^{2HDM} = \frac{-3e}{m_W s_W s_{2\beta}^2} \left[(c_\beta c_\alpha^3 - s_\beta s_\alpha^3) s_{2\beta} m_{H^0}^2 - s_{\beta-\alpha}^2 s_{\beta+\alpha} m_{12}^2 \right] \quad (6)$$

$$\lambda_{H^0 h^0 h^0}^{2HDM} = -\frac{1}{2} \frac{ec_{\beta-\alpha}}{m_W s_W s_{2\beta}^2} \left[(2m_{h^0}^2 + m_{H^0}^2) s_{2\alpha} s_{2\beta} - (3s_{2\alpha} - s_{2\beta}) m_{12}^2 \right] \quad (7)$$

$$\lambda_{H^0 H^0 h^0}^{2HDM} = \frac{1}{2} \frac{es_{\beta-\alpha}}{m_W s_W s_{2\beta}^2} \left[(m_{h^0}^2 + 2m_{H^0}^2) s_{2\alpha} s_{2\beta} - (3s_{2\alpha} + s_{2\beta}) m_{12}^2 \right] \quad (8)$$

$$\lambda_{A^0 A^0 h^0}^{2HDM} = \frac{-e}{m_W s_W s_{2\beta}^2} \left[(c_\alpha c_\beta^3 - s_\alpha s_\beta^3) s_{2\beta} m_{h^0}^2 - c_{\beta+\alpha} m_{12}^2 + s_{2\beta}^2 s_{\beta-\alpha} m_{A^0}^2 \right] \quad (9)$$

$$\lambda_{A^0 A^0 H^0}^{2HDM} = \frac{-e}{m_W s_W s_{2\beta}^2} \left[(s_\alpha c_\beta^3 + c_\alpha s_\beta^3) s_{2\beta} m_{H^0}^2 - s_{\beta+\alpha} m_{12}^2 + s_{2\beta}^2 c_{\beta-\alpha} m_{A^0}^2 \right] \quad (10)$$

$$\lambda_{A^0 G^0 h^0}^{2HDM} = \frac{1}{2} \frac{ec_{\beta-\alpha}}{m_W s_W} (m_{A^0}^2 - m_{h^0}^2) \quad (11)$$

$$\lambda_{A^0 G^0 H^0}^{2HDM} = -\frac{1}{2} \frac{es_{\beta-\alpha}}{m_W s_W} (m_{A^0}^2 - m_{H^0}^2) \quad (12)$$

$$\lambda_{H^\pm H^\mp h^0}^{2HDM} = \frac{e}{m_W s_W s_{2\beta}^2} \left[(s_\alpha s_\beta^3 - c_\alpha c_\beta^3) s_{2\beta} m_{h^0}^2 + c_{\beta+\alpha} m_{12}^2 - s_{2\beta}^2 s_{\beta-\alpha} m_{H^\pm}^2 \right] \quad (13)$$

$$\lambda_{H^\pm H^\mp H^0}^{2HDM} = \frac{-e}{m_W s_W s_{2\beta}^2} \left[(s_\alpha c_\beta^3 + s_\alpha s_\beta^3) s_{2\beta} m_{H^0}^2 - s_{\beta+\alpha} m_{12}^2 + s_{2\beta}^2 c_{\beta-\alpha} m_{H^\pm}^2 \right] \quad (14)$$

where $\lambda_{h^0 h^0 h^0}^{SM}$ is the SM triple Higgs coupling. Here we use the short-hand notations: $s_W = \sin\theta_W$ with θ_W being the weak mixing angle, and s_ϕ and c_ϕ denote respectively $\sin\phi$ and $\cos\phi$ for ϕ being various linear combinations of α and β .

As we can see from Eqs. (5)-(14), all triple Higgs couplings have some quadratic dependence on the physical masses m_Φ and soft breaking term m_{12} . These couplings also depend strongly on $\tan\beta$ and α . In the present study, we will show that varying the scalar parameters within the allowed range can still make the triple Higgs couplings larger than the SM triple Higgs coupling $\lambda_{h^0 h^0 h^0}^{SM} = -3em_{h^0}^2/(2m_W s_W)$ by several orders of magnitude. These 2HDM triple Higgs couplings can also be large compared to the MSSM triple Higgs couplings. The reason for this is that in the MSSM, supersymmetry imposes restrictions on the quartic couplings λ_i by relating them to the gauge couplings [6, 8].

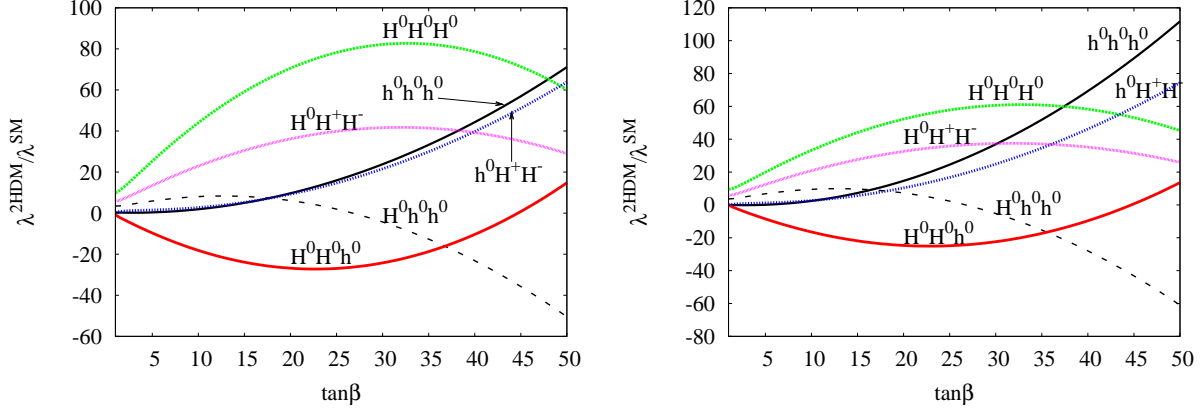


FIG. 3: The 2HDM tree level self couplings $\lambda_{h_i h_j h_k}^{2HDM}$ normalized to the SM self coupling λ_{hhh}^{SM} as a function of $\tan\beta$. The plots use $m_{h^0} = 120$ GeV, $m_{H^0} = 370$ GeV, $m_{A^0} = 150$ GeV, $m_{H^\pm} = 250$ GeV, $m_{12} = 46$ GeV, $\sin\alpha = 0.6$ (left panel) and $\sin\alpha = 0.7$ (right panel).

Taking into account all the previous theoretical and experimental constraints listed in the above subsection, we give here the sizes of the triple Higgs couplings involved in the double Higgs-strahlung production.

In Fig. 2, we illustrate the sizes of the triple Higgs couplings as a function of CP-even Higgs mass m_{H^0} (left plot) and as a function of the discrete symmetry breaking parameter m_{12} (right plot). One can see from these plots that the sizes of triple Higgs couplings normalized to the SM triple Higgs coupling lie between -10 and 12 for all allowed values of m_{H^0} and m_{12} .

If the splitting between H^\pm and A^0 is small, it follows from Eqs. (9) and (13) [Eqs. (10) and (14)] the couplings $\lambda_{h^0 A^0 A^0}$ and $\lambda_{h^0 H^+ H^-}$ [$\lambda_{H^0 A^0 A^0}$ and $\lambda_{H^0 H^+ H^-}$] are almost equal. The couplings $\lambda_{h^0 H^+ H^-}$ and $\lambda_{H^0 H^+ H^-}$ are thus not shown. It is clear from Eqs. (5) and (10) that $\lambda_{h^0 h^0 h^0}$ and $\lambda_{h^0 A^0 A^0}$ have no m_{H^0} dependence. That is why $\lambda_{h^0 h^0 h^0}$ and $\lambda_{h^0 A^0 A^0}$ exhibit no variation over m_{H^0} . For the other couplings, the variation over m_{H^0} can change the size of these couplings by about one order of magnitude.

The dependence of the triple Higgs couplings on m_{12} is also important (see the right plot of Fig. 2). However, due to the perturbativity and vacuum stability conditions, m_{12} is constrained to be less than 55 GeV. It is interesting to note that the couplings $\lambda_{h^0 h^0 h^0}$ and $\lambda_{H^0 h^0 h^0}$ contributing to $e^+ e^- \rightarrow Z h^0 h^0$ enter with opposite signs and may have a destructive interference in the amplitude. The same observation holds for $\lambda_{h^0 A^0 A^0}$, $\lambda_{H^0 A^0 A^0}$, $\lambda_{h^0 H^+ H^-}$

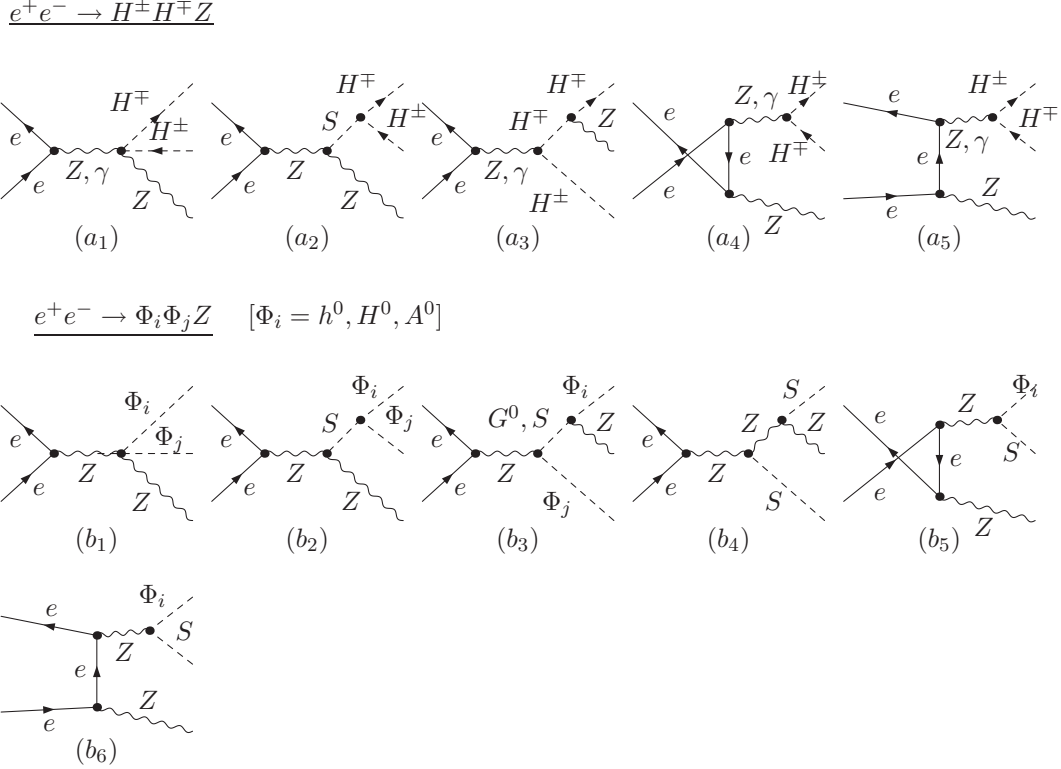


FIG. 4: Double charged and neutral Higgs-strahlung production in the 2HDM at e^+e^- linear colliders with $S = h^0$ or H^0 .

and $\lambda_{H^0 H^+ H^-}$.

In Fig. 3, we show the variation of triple Higgs couplings as a function of $\tan \beta$. We fix $m_{12} = 46$ GeV, $m_{h^0} = 120$ GeV, $m_{H^0} = 370$ GeV, $m_{A^0} = 150$ GeV, $m_{H^\pm} = 250$ GeV, and $\sin \alpha = 0.6$ for left panel and $\sin \alpha = 0.7$ for right panel. Almost all the triple Higgs couplings are enhanced in the large $\tan \beta$ limit. The triple Higgs couplings $\lambda_{H^0 H^0 H^0}$, $\lambda_{h^0 h^0 h^0}$, $\lambda_{H^0 h^0 h^0}$ and $\lambda_{h^0 H^+ H^-}$ can be more than 50 times larger than the SM triple coupling. This $\tan \beta$ effect has been first noticed in Refs. [14, 33]. It is also worth pointing out that some of the 2HDM couplings $\lambda_{h_i h_j h_k}$ can flip sign as one varies m_{12} and/or $\tan \beta$.

Note that only in Fig. 3 we ignore perturbativity and vacuum stability constraints. In fact, in the left panel (right panel), perturbativity constraints are violated for $6 \lesssim \tan \beta \lesssim 49$ ($7.5 \lesssim \tan \beta \lesssim 48$) while vacuum stability constraints are violated for $43 \lesssim \tan \beta \lesssim 49$ ($36 \lesssim \tan \beta \lesssim 50$).

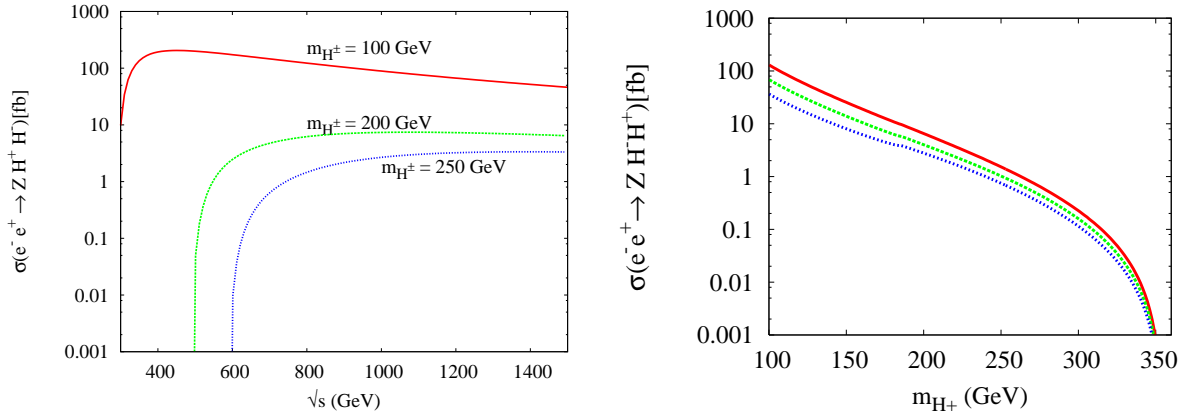


FIG. 5: $\sigma(e^+e^- \rightarrow H^+H^-Z)$ in units of fb as a function of center-of-mass energy (left) for several values of m_{H^\pm} and as a function m_{H^\pm} (right) for $\sqrt{s} = 800$ GeV. Regarding the other parameters, the left plot uses $m_{h^0} = 120$ GeV, $m_{H^0} = 370$ GeV, $m_{12} = 45$ GeV, $m_{A^0} = 150$ GeV, $\tan\beta = 53$ and $\cos(\beta - \alpha) = 0.5$. From top to bottom in the right plot, $(\tan\beta, m_{12}) = (55, 44)$ GeV, $(40, 52)$ GeV, and $(30, 60)$ GeV).

III. PROBING TRIPLE COUPLINGS FROM DOUBLE HIGGS-STRAHLUNG PROCESSES

A. $e^+e^- \rightarrow \Phi_i\Phi_jZ$

In this section we will cover the following processes: $e^+e^- \rightarrow H^+H^-Z$, $e^+e^- \rightarrow h^0h^0Z$, $e^+e^- \rightarrow h^0H^0Z$, $e^+e^- \rightarrow H^0H^0Z$, and $e^+e^- \rightarrow A^0A^0Z$. The two processes $e^+e^- \rightarrow h^0A^0Z$ and $e^+e^- \rightarrow H^0A^0Z$ are not sensitive to any triple Higgs couplings; they proceed only through gauge couplings and will not be calculated here.

Measurements of those processes will give some information on the involved triple Higgs couplings. The complete calculation is done with the packages FeynArts [34], FormCalc [35], and LoopTools [36]. In these $2 \rightarrow 3$ processes, a width for the internal Higgs exchange is needed to stabilize the phase space integration. Such a width is introduced and computed at the tree level. The numerical evaluations of the integration over $2 \rightarrow 3$ phase space is done with the help of CUBA library [37].

Before discussing our numerical results, it is worth pointing out that the following results are valid for both 2HDM-I and 2HDM-II since they involve only the Higgs coupling and the gauge coupling to Higgs or to e^+e^- .

Feynman diagrams for the first process $e^+e^- \rightarrow H^+H^-Z$ are depicted in the first set of Fig. 4. Only diagram (a_2) is sensitive to the triple Higgs couplings $\lambda_{h^0H^+H^-}$ and $\lambda_{H^0H^+H^-}$. The other diagrams proceed through gauge interactions only. Similarly, Feynman diagrams for the processes $e^+e^- \rightarrow \Phi_i\Phi_jZ$ with $\Phi_i = h^0, H^0, A^0$ are depicted in the second set of Fig. 4. As we can see, only diagram (b_2) has a triple Higgs couplings dependence. The other diagrams depend only on gauge couplings.

To illustrate the size of $e^+e^- \rightarrow H^+H^-Z$ cross section, we show in Fig. 5 $\sigma(e^+e^- \rightarrow H^+H^-Z)$ as a function of center-of-mass energy for $m_{H^\pm} = 100, 150, 200$ GeV. The cross section exceeds 100 fb for light charged Higgs mass of 100 GeV. For moderate charged Higgs mass of 200 GeV, the cross section is still of the order of a few fb.

In the right panel of Fig. 5, we illustrate the sensitivity of the cross section to m_{H^\pm} for a fixed center-of-mass energy of 800 GeV. By varying m_{H^\pm} from 100 to 350 GeV, the cross section is suppressed by several orders of magnitude. However, for a charged Higgs mass in the range 100 to 300 GeV, it is still possible to have a total cross section larger than 0.1 fb. This can lead to 100 raw events for the planned luminosity of 1000 fb^{-1} .

The collider signature for the $e^+e^- \rightarrow H^+H^-Z$ process depends on how H^\pm decays. Below the top-bottom threshold and before the charged Higgs to neutral Higgs decays $H^\pm \rightarrow SW^\pm$ ($S = h^0, A^0$) are open, the signature would be $Z\tau^+\tau^- + \cancel{E}_T$ or $Zc\bar{s}c\bar{s}$. Once the charged Higgs to neutral Higgs decays $H^\pm \rightarrow W^\pm S$ become open, one would get the ZW^+W^-SS final states with S decaying either to $b\bar{b}$ or $\tau^+\tau^-$. Above the top-bottom threshold, the signature would be $Zt\bar{t}b\bar{b}$ if $Br(H^\pm \rightarrow t\bar{b})$ dominates or ZW^+W^-SS if $Br(H^\pm \rightarrow W^\pm S)$ dominates.

Let us now turn to double Higgs-strahlung processes $e^+e^- \rightarrow \Phi_i\Phi_jZ$, with $\Phi_{i,j}$ being neutral Higgs bosons h^0, H^0, A^0 . As noted in the previous section, the $\Phi_iH^+H^-$ and $\Phi_iA^0A^0$ couplings ($\Phi_i = h^0, H^0$) are almost identical for not too large mass splitting between charged and CP-odd Higgs. As we will see, the total cross section of $e^+e^- \rightarrow ZA^0A^0$ has similar behavior and size to the total cross section of $e^+e^- \rightarrow H^+H^-Z$ for m_{A^0} and m_{H^\pm} of about the same magnitude.

In Fig. 6, we show the total cross sections for the neutral modes $Zh^0h^0, Zh^0H^0, ZH^0H^0$ and ZA^0A^0 as a function of the center-of-mass energy \sqrt{s} for different values of m_{A^0} . As explained in the figure caption, we select specific $\sin\alpha$ values to optimize the total cross sections. The behavior of the cross section for those neutral modes is similar to that of

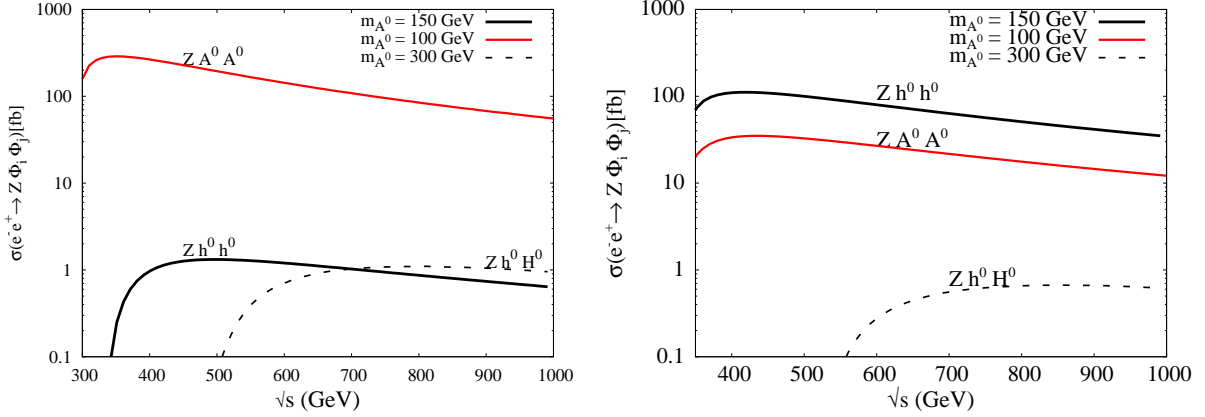


FIG. 6: Total tree level cross section of $e^+e^- \rightarrow Z\Phi_i\Phi_i$ in 2HDM as a function of \sqrt{s} with $m_{h^0} = 120$ GeV, $m_{H^\pm} = 140$ GeV, $m_{12} = 0$ GeV, $\tan\beta = 10$ for different values of m_{A^0} . The left plot uses $m_{H^0} = 200$ GeV and $\sin\alpha = 0.6$. The right plot uses $m_{H^0} = 240$ GeV and $\sin\alpha = 0.8$.

$e^+e^- \rightarrow ZH^+H^-$. The reasons are that for both processes we have similar topologies in the contributing Feynman diagrams and that the triple Higgs couplings have a similar magnitude. For the Zh^0h^0 and ZA^0A^0 modes, the total cross section is maximized for $\sqrt{s} \approx 350 - 400$ GeV. In the case of Zh^0h^0 with $m_{h^0} = 120$ GeV, the maximum of the total cross section is reached for $m_{A^0} = 150$ GeV, $m_{H^0} = 240$ GeV, and $\sin\alpha = 0.8$ (right panel), and is slightly larger than 100 fb. This enhancement for $e^+e^- \rightarrow Zh^0h^0$ is due to the threshold effect ($H^0 \rightarrow h^0h^0$ is open). In the ZA^0A^0 mode, the cross section is maximal for $m_{A^0} = 150$ GeV, $m_{H^0} = 200$ GeV, and $\sin\alpha = 0.6$ and is about 300 fb. The cross section of the heavy mode ZH^0H^0 is very small and is not shown; whereas the cross section of the mixed mode ZH^0h^0 is mild, ≈ 1 fb, in both cases.

In order to show the sensitivity of the cross sections to high $\tan\beta$, we plot in Fig. 7 the cases of small $\tan\beta$ (left) and large $\tan\beta$ (right). For small $\tan\beta$, $e^+e^- \rightarrow ZA^0A^0$ dominates with a few fb cross section, $e^+e^- \rightarrow Zh^0h^0$ and $e^+e^- \rightarrow Zh^0H^0$ barely reaches 0.1 fb. This is due to the fact that the triple Higgs couplings involved in these processes are such that

$$(\lambda_{h^0h^0h^0}^{2HDM}, \lambda_{H^0h^0h^0}^{2HDM}, \lambda_{h^0A^0A^0}^{2HDM}, \lambda_{H^0A^0A^0}^{2HDM}) \approx (0.6, 5, 0.4, 13) \times \lambda_{h^0h^0h^0}^{SM}.$$

They are not enhanced by much except for $\lambda_{H^0A^0A^0}$ which is $13\lambda_{h^0h^0h^0}^{SM}$ and explains the dominance of $e^+e^- \rightarrow ZA^0A^0$ in this case. However, in large $\tan\beta$ cases, $e^+e^- \rightarrow Zh^0h^0$ has the largest cross section (≈ 60 fb), followed by $e^+e^- \rightarrow ZA^0A^0$ (≈ 20 fb). In this large

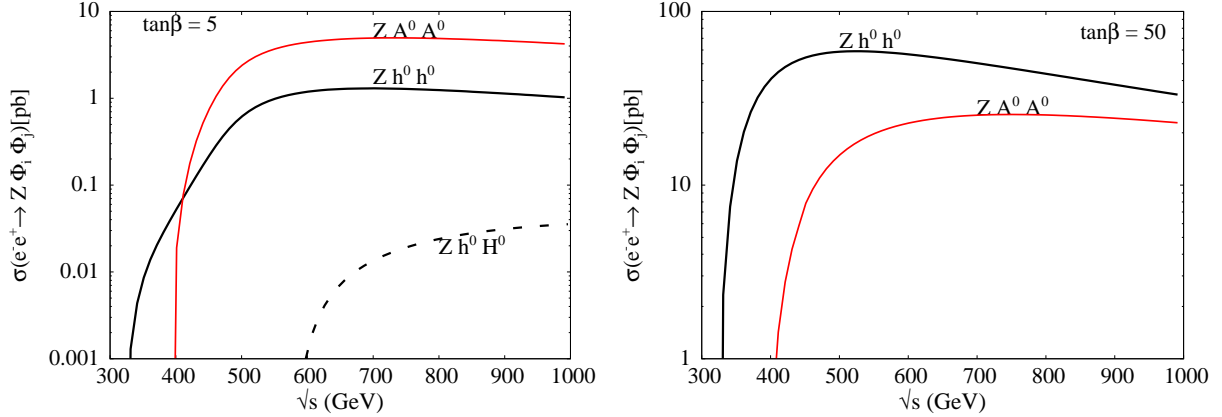


FIG. 7: Total tree level cross sections of $e^+e^- \rightarrow Z\Phi_i\Phi_i$ in 2HDM as a function of \sqrt{s} with $m_{h^0} = 120$ GeV, $m_{H^0} = 370$ GeV, $m_{H^\pm} = 250$ GeV, $m_{A^0} = 150$ GeV, $m_{12} = 46$ GeV, $\sin\alpha = 0.6$ and $\tan\beta = 5$ (left) or $\tan\beta = 50$ (right).

$\tan\beta$ case, the involved triple Higgs couplings are given by

$$(\lambda_{h^0h^0h^0}^{2HDM}, \lambda_{H^0h^0h^0}^{2HDM}, \lambda_{h^0A^0A^0}^{2HDM}, \lambda_{H^0A^0A^0}^{2HDM}) \approx (43, -39, 52, 30) \times \lambda_{h^0h^0h^0}^{SM}.$$

Obviously, they are much more enhanced than the low $\tan\beta$ case.

Fig. 8 shows the behaviors of $e^+e^- \rightarrow Zh^0h^0$ and $e^+e^- \rightarrow ZA^0A^0$ (left plot) and the branching ratios of the CP-even H^0 (right plot) as a function of m_{H^0} and for $m_{h^0}, m_{H^\pm}, m_{A^0}, m_{12} = 120, 250, 150, 0$ GeV, respectively, $\tan\beta = 5$, $\sin\alpha = 0.9$ and $\sqrt{s} = 500$ GeV. To compute the cross sections, we have summed the continuum part $\sigma(e^+e^- \rightarrow ZSS)$ and resonant part generated in the chain $e^+e^- \rightarrow ZH^0 \rightarrow ZSS$ via the resonant H^0 Higgsstrahlung, with $S = h^0$ or A^0 . It is obvious that the cross sections of $e^+e^- \rightarrow Zh^0h^0$ and $e^+e^- \rightarrow ZA^0A^0$ reach their maxima near the threshold regions of $H^0 \rightarrow h^0h^0$ and $H^0 \rightarrow A^0A^0$.

In the right panel of Fig. 8, we show the decay branching ratios of H^0 . The $b\bar{b}$ mode dominates below the WW threshold, while the WW mode takes over for $m_{H^0} \gtrsim 2M_W$. Above the h^0h^0 threshold, the decay $H^0 \rightarrow h^0h^0$ is open and dominates over the others at the order of 70%. For $m_{H^0} \gtrsim 300$ GeV, $H^0 \rightarrow A^0A^0$ is open and has also a substantial branching ratio of $\mathcal{O}(20\%)$, reducing the branching ratio of $H^0 \rightarrow h^0h^0$ to the level of less than 20%. Note that once $H^0 \rightarrow H^+H^-$ is open, it quickly reaches the level of 15%.

As shown in the left plot of Fig. 8, there are three kinks occurring when $m_{H^0} = 2m_{h^0}, 2m_{A^0}, 2m_{H^\pm}$ and corresponding to the opening of the $H^0 \rightarrow h^0h^0, H^0 \rightarrow A^0A^0$ and

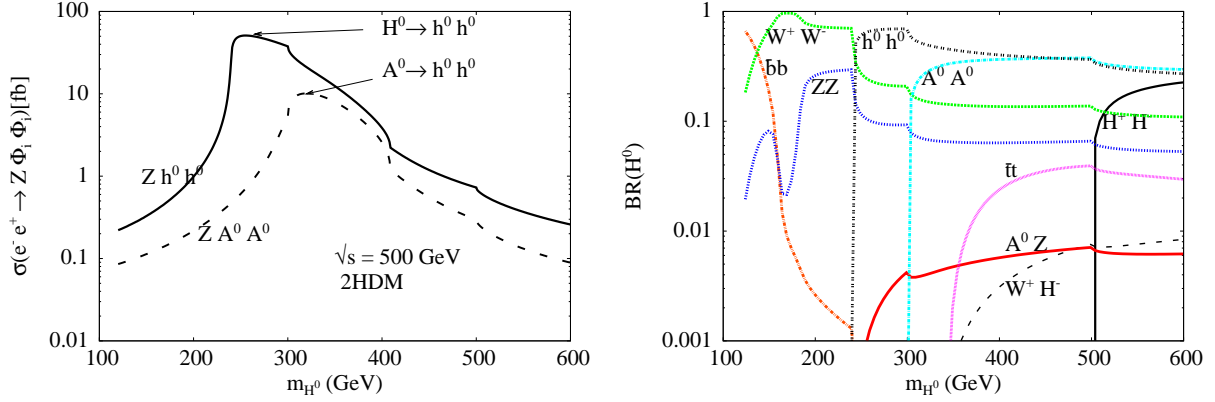


FIG. 8: Left plot: total cross sections for Zh^0h^0 and ZA^0A^0 continuum and resonant production: $\sigma(e^+e^- \rightarrow Zh^0h^0) + \sigma(e^+e^- \rightarrow ZH^0) \cdot BR(H^0 \rightarrow h^0h^0, A^0A^0)$ in 2HDM as a function of m_{H^0} . Right plot: branching ratios of H^0 . Here $m_{h^0} = 120$ GeV, $m_{H^\pm} = 250$ GeV, $m_{A^0} = 150$ GeV, $m_{12} = 0$ GeV, $\tan\beta = 5$, and $\sin\alpha = 0.9$.

$H^0 \rightarrow H^\pm H^\mp$ modes, respectively. The cross sections increase by about 20 fb if h^0h^0 and A^0A^0 are produced in $e^+e^- \rightarrow ZH^0 \rightarrow Zh^0h^0$ and $e^+e^- \rightarrow ZH^0 \rightarrow Zh^0h^0$ via resonant Higgs-strahlung of H^0 .

For the double Higgs-strahlung processes $e^+e^- \rightarrow Zh^0h^0$, $e^+e^- \rightarrow ZA^0A^0$ and $e^+e^- \rightarrow ZH^0H^0$, the dominant final states depend on how h^0 , A^0 and H^0 decay. In the case where h^0 and A^0 are not heavy ($\lesssim 125$ GeV), h^0 and A^0 will decay to $b\bar{b}$ or $\tau^+\tau^-$, and the final states for Zh^0h^0 and ZA^0A^0 would be $Z4b$, $Z2b2\tau$ or $Z4\tau$. In the 2HDM, it may be possible that, if kinematically allowed, A^0 decays into Zh^0 . In this case, the final state for ZA^0A^0 would be $ZA^0A^0 \rightarrow 3Zh^0h^0 \rightarrow 3Z4b$. For the $e^+e^- \rightarrow Zh^0H^0$ process, the final state will be different from the previous one if the Higgs to Higgs decays $H^0 \rightarrow h^0h^0$ and $H^0 \rightarrow A^0A^0$ are open. As a result, the final state would be $Zh^0h^0h^0$ and $Zh^0A^0A^0$.

We would like to stress here that the background study is beyond the scope of this paper. However, we point out that in the SM with small cross sections, it has been shown in Ref. [10] that for the $e^+e^- \rightarrow ZHH \rightarrow Zb\bar{b}b\bar{b}$ process in the SM, the irreducible background from electroweak and QCD processes can be suppressed down to manageable levels by using kinematics cuts. We expect that in the 2HDM with larger cross sections than in SM, the signal can be easily extracted from the background as well.

B. Double Higgs-strahlung in the fermiophobic limit

As commented in Section 2, in 2HDM-I the lightest CP-even Higgs boson h^0 can be fermiophobic [4, 21]. This occurs when $\alpha = \pi/2$ ($\cos \alpha = 0$), so that the lightest Higgs couplings to all fermions vanish. In this case, the main decay channel of h^0 ($m_{h^0} < 2M_W$) is $h^0 \rightarrow \gamma\gamma$ for $m_{h^0} < M_V$ and $h^0 \rightarrow VV^*$ for $m_{h^0} > m_V$, where $V = W, Z$ [4, 38]. Once the WW threshold is crossed, the dominant decay mode becomes $h^0 \rightarrow W^+W^-$.

The LEP Collaboration has already ruled out a fermiophobic Higgs with a mass $m_{h^0} \lesssim 104$ GeV and the ZZh^0 coupling similar to the SM one [39]. This constraint can be lifted if the ZZh^0 coupling is smaller than the SM one.

Recently, there is a study devoted to double fermiophobic Higgs bosons production at the LHC and ILC [40]. For the ILC, it has been shown that $e^+e^- \rightarrow A^0h^0$ followed by the decay $A^0 \rightarrow Zh^0$ can lead to the Zh^0h^0 final state that is similar to our double Higgs-strahlung process $e^+e^- \rightarrow Zh^0h^0$. However, the process $A^0h^0 \rightarrow Zh^0h^0$ only depends on the gauge couplings while the double Higgs-strahlung process $e^+e^- \rightarrow Zh^0h^0$ under consideration is sensitive to the 2HDM triple Higgs couplings that may enhance the cross section.

In Fig. 9, we show the total cross sections of the neutral modes Zh^0h^0 and Zh^0H^0 in the fermiophobic limit $\sin \alpha = 1$ for a relatively light CP-even fermiophobic Higgs with $m_{h^0} = 80$ GeV. This possibility is not yet ruled out experimentally [39] due to suppressed ZZh^0 coupling. This fermiophobic limit is only relevant for final states having at least one fermiophobic Higgs, namely the $e^+e^- \rightarrow Zh^0h^0$ and $e^+e^- \rightarrow Zh^0H^0$ modes where the h^0 may decay dominantly into two photons. In the left panel of Fig. 9 we select moderate $\tan \beta = 10$, and the right panel is for small $\tan \beta = 1$. For both channels, Zh^0h^0 and Zh^0H^0 , the cross sections are of the order of few fb and can reach 20 fb (10fb) for Zh^0h^0 in the case of $\tan \beta = 10$ ($\tan \beta = 1$). Due to phase space suppression, the cross section of $e^+e^- \rightarrow Zh^0H^0$ is smaller than $e^+e^- \rightarrow Zh^0h^0$.

In the fermiophobic limit of 2HDM-I, one can obtain a very clear signal of $4\gamma + X$ from the Zh^0h^0 mode. For the Zh^0H^0 mode, the signal depends on how H^0 decays. In 2HDM, the heavy Higgs H^0 can decay to W^+W^- or, if kinematically allowed, to h^0h^0 . In the latter case, we have $ZH^0h^0 \rightarrow Zh^0h^0h^0 \rightarrow Z6\gamma$ with $6\gamma + X$ as a distinctive signature.

To our best knowledge, there is no estimation for the $e^+e^- \rightarrow 4\gamma Z$ backgrounds. We expect that such backgrounds should be small. Moreover, requesting four photons in our

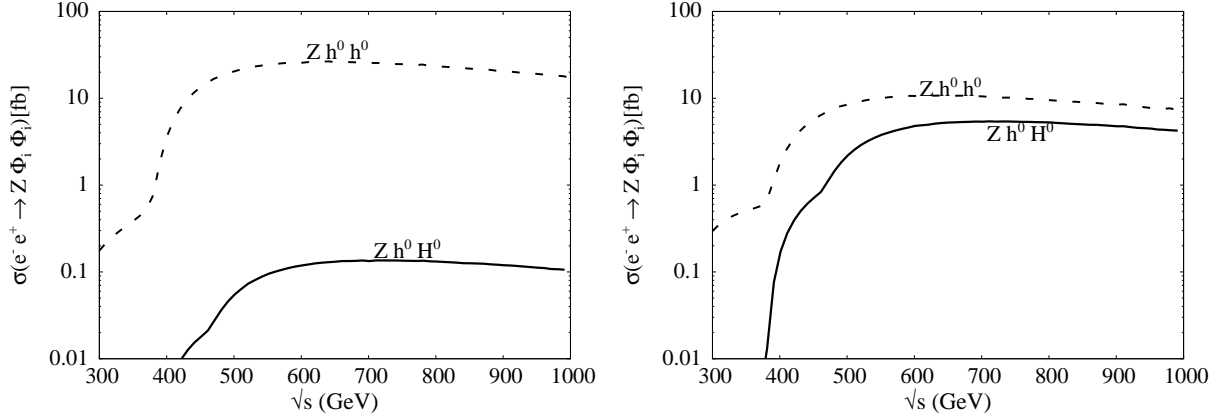


FIG. 9: The tree level cross sections of the $e^+e^- \rightarrow Zh^0h^0, Zh^0H^0$ processes as a function of the center-of-mass energy in the fermiophobic limit with $m_{12} = 0$ GeV, $m_{h^0} = 80$ GeV, $m_{H^0} = 160$ GeV, $m_{A^0} = 300$ GeV, $m_{H^\pm} = 250$ GeV, and $\tan\beta = 10$ (left) or $\tan\beta = 1$ (right).

signal would be sufficient to kill the backgrounds.

C. $e^+e^- \rightarrow h^0h^0Z$ in the decoupling limit

In the 2HDM, the decoupling limit generally refers to the case when all the scalar masses except one formally become infinite and the effective theory is just the SM with one doublet (see [15] for recent discussions). In this case, the CP-even h^0 is the lightest scalar particle while the other Higgs particles H^0 , A^0 and H^\pm are extremely heavy. Using purely algebraic arguments at the tree level, one can derive that the main consequences of the decoupling limit are $\cos(\beta - \alpha) \rightarrow 0$, and the CP-even h^0 of the 2HDM and the SM Higgs h_{SM} have similar tree-level couplings to gauge bosons and fermions as well [15, 43]. Obviously, the decoupling limit does not rigorously apply to the cases where the particle masses are finite. One can consider instead a more realistic scenario, dubbed as the decoupling regime [15], where the heavy Higgs particles have masses much larger than the Z boson mass and may escape detection in the planned experiments.

Several studies have been carried out looking for non-decoupling effects in Higgs boson decays and Higgs self-interactions. Large loop effects in $h^0 \rightarrow \gamma\gamma$, $h^0 \rightarrow \gamma Z$ and $h^0 \rightarrow b\bar{b}$ have been pointed out for the 2HDM [41, 42] and may provide indirect information on the Higgs masses and the involved triple Higgs couplings such as $\lambda_{h^0H^+H^-}$, $\lambda_{h^0H^0H^0}$, $\lambda_{h^0A^0A^0}$ and $\lambda_{h^0h^0h^0}$. The non-decoupling contributions to the triple Higgs self-couplings $\lambda_{h^0h^0h^0}$ have

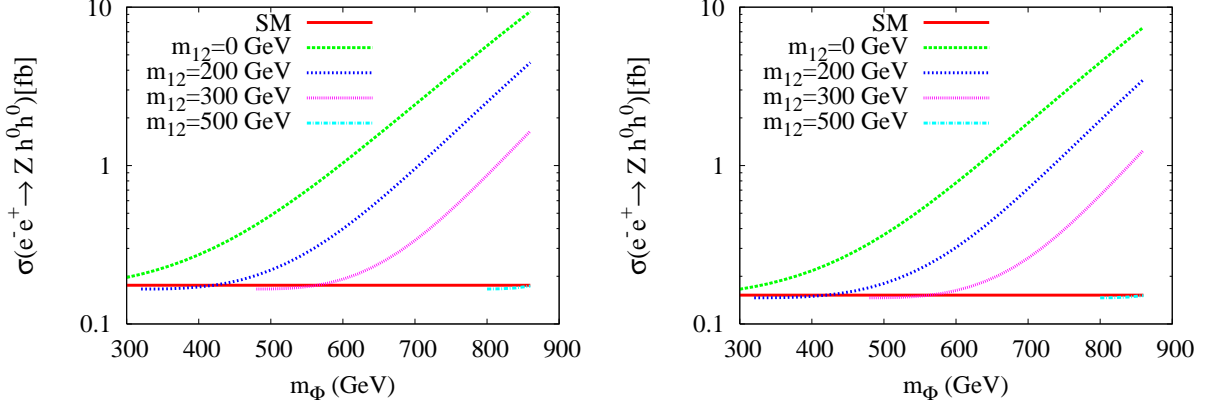


FIG. 10: $\sigma(e^+e^- \rightarrow Zh^0h^0)$ in units of fb as a function of M_Φ at $\sqrt{s} = 500$ GeV (left) and $\sqrt{s} = 800$ GeV (right) for different values of m_{12} . For both plots, $m_{h^0} = 120$ GeV, $\tan\beta = 2$ and $\cos(\beta - \alpha) = 0$.

been investigated in the 2HDM in Ref. [43], revealing large non-decoupling effects.

In this section, we will show that the large non-decoupling effects in $\lambda_{h^0h^0h^0}$ modify the double Higgs-strahlung $e^+e^- \rightarrow Zh^0h^0$ cross section and make it larger than the SM expectation. We will focus on the scenario where all the Higgs particles of the 2HDM, except for the lightest CP-even Higgs, are heavy and can escape from detection at the first stage of next generation colliders.

It is easy to check that in the decoupling limit $\beta - \alpha \rightarrow \pi/2$, the triple Higgs coupling $\lambda_{h^0h^0h^0}$ given in Eq. (5) reduces to its SM value $\lambda_{h^0h^0h^0}^{SM} = -3m_{h^0}^2/v$. In Ref. [43], using the Feynman diagrammatic method, it has been demonstrated that the one-loop leading contributions originated from the heavy Higgs boson loops and the top quark loops to the effective $\lambda_{h^0h^0h^0}$ coupling can be written as

$$\lambda_{h^0h^0h^0}^{eff}(2HDM) = \frac{3m_{h^0}^2}{v} \left\{ 1 + \frac{m_{H^0}^4}{12\pi^2 m_{h^0}^2 v^2} \left(1 - \frac{M^2}{m_{h^0}^2} \right)^3 + \frac{m_{A^0}^4}{12\pi^2 m_{h^0}^2 v^2} \left(1 - \frac{M^2}{m_{A^0}^2} \right)^3 + \frac{m_{H^\pm}^4}{6\pi^2 m_{h^0}^2 v^2} \left(1 - \frac{M^2}{m_{H^\pm}^2} \right)^3 - \frac{N_c m_t^4}{3\pi^2 m_{h^0}^2 v^2} + \mathcal{O} \left(\frac{p_i^2 m_\Phi^2}{m_{h^0}^2 v^2}, \frac{m_\Phi^2}{v^2}, \frac{p_i^2 m_t^2}{m_{h^0}^2 v^2}, \frac{m_t^2}{v^2} \right) \right\}, \quad (15)$$

where $M = m_{12}/\sqrt{\sin\beta \cos\beta}$, m_Φ and p_i represent the mass of H^0 , A^0 or H^\pm and the momenta of external Higgs lines, respectively, N_c denotes the number of colors, and m_t is the mass of top quark. We note that in Eq. (15) m_{h^0} is the renormalized physical mass of the lightest CP-even Higgs boson h^0 .

At the tree level, one can show that in the decoupling limit the ZZH^0 coupling approaches 0 and the $e^+e^- \rightarrow Zh^0h^0$ amplitude reduces exactly to the SM result. For our calculation of the cross section of $e^+e^- \rightarrow Zh^0h^0$ in the decoupling limit, we ignore one-loop corrections to the ZZh^0 coupling and replace the $h^0h^0h^0$ coupling by its effective coupling given in Eq. (15). In fact, it has been shown in Ref. [43] that the non-decoupling effect in ZZh^0 is at a few percent level in the case of $\cos(\beta - \alpha) = 0$.

In Fig. 10, we show the cross section of $e^+e^- \rightarrow Zh^0h^0$ in the SM and 2HDM in its decoupling regime as a function of $m_\Phi = m_{A^0} = m_{H^0} = m_{H^\pm}$. In the calculation of the SM cross section, we take into account the one-loop leading contributions originated from top quarks given by [43]

$$\lambda_{hhh}^{eff}(SM) = \frac{3m_{h^0}^2}{v} \left\{ 1 - \frac{N_c m_t^4}{3\pi^2 m_{h^0}^2 v^2} + \mathcal{O}\left(\frac{m_t^2}{v^2}\right) \right\}, \quad (16)$$

For our choice of $m_{h^0} = 120$ GeV, the SM cross section is tiny, ≈ 0.2 fb and 0.16 fb for $\sqrt{s} = 500, 800$ GeV, respectively. As is clear in Fig. 10, the 2HDM contributions can enhance the cross section by more than one order of magnitude and reach a few fb for small m_{12} and large m_Φ . As shown in both panels of Fig. 10, we get maximum non-decoupling effect for $m_{12} = 0$. It is further amplified with large m_Φ . The plots are cut due to the perturbativity and vacuum stability constraints. The perturbativity constraints on λ_i do not allow m_Φ larger than 850 GeV. In the case of $m_{12} = 500$ GeV, the vacuum stability condition does not allow m_Φ to be less than 800 GeV. The sensitivity of cross section to $\tan\beta$ is mild, since $\tan\beta$ only enters the $h^0h^0h^0$ coupling through $M^2 = m_{12}^2/(\sin\beta\cos\beta)$. Moreover, $\tan\beta$ is constrained by perturbativity to be rather moderate.

IV. SUMMARY

We have studied the triple Higgs couplings $\lambda_{\Phi_i\Phi_j\Phi_k}$ and the double Higgs-strahlung production $e^+e^- \rightarrow Z\Phi_i\Phi_j$ at linear collider in the framework of general Two Higgs Doublet Models. We have quantified the sizes of the triple Higgs couplings compared to the SM triple Higgs coupling. We also show that after taking into account the perturbativity and vacuum stability constraints on the 2HDM parameters, it is possible to enhance the triple Higgs coupling $\lambda_{h^0h^0h^0}$ up to 15 times or more than the corresponding SM coupling. If the Higgs bosons $\Phi = h^0, H^0, A^0$ and H^\pm are not too heavy, the double Higgs-strahlung cross

sections $e^+e^- \rightarrow Z\Phi_i\Phi_j$ can be substantial, at the level of a few hundred fb, and provide some information on the triple Higgs couplings.

We have also studied the double Higgs-strahlung processes $e^+e^- \rightarrow Zh^0h^0$ and $e^+e^- \rightarrow ZH^0h^0$ in the fermiophobic limit of 2HDM-I where the collider signature can be very distinctive with the final state $Z2\gamma$, $Z4\gamma$, or $Z6\gamma$ if $H^0 \rightarrow h^0h^0$. We also analyze the double Higgs-strahlung process $e^+e^- \rightarrow Zh^0h^0$ in the decoupling limit where h^0 mimics the SM Higgs boson. It is shown that in this limit, the cross section can be enhanced by about two orders of magnitude, which is much larger than the MSSM enhancement. Observations of such large cross sections would definitely indicate that the Higgs sector is 2HDM-like.

V. ACKNOWLEDGMENTS

We would like to thank A.G. Akeroyd, S. Kanemura, R.R. Santos and Eibun Senaha for valuable discussions and comments. AA, RB and CWC are supported by the National Science Council of R.O.C. under Grant Nos. NSC 96-2811-M-008-020, NSC 96-2811-M-033-005, and NSC 96-2112-M-008-001, respectively. CWC also thanks the Institute of Physics at National Chiao-Tung Univ. for the hospitality during his visit.

-
- [1] P. W. Higgs, Phys. Rev. Lett. **13** (1964) 508. G. S. Guralnik, C. R. Hagen and T. W. B. Kibble, Phys. Rev. Lett. **13**, 585 (1964). F. Englert and R. Brout, Phys. Rev. Lett. **13** (1964) 321.
 - [2] M. Duhrssen, S. Heinemeyer, H. Logan, D. Rainwater, G. Weiglein and D. Zeppenfeld, Phys. Rev. D **70** (2004) 113009 [arXiv:hep-ph/0406323]; C. Ruwiedel and f. t. A. Collaborations, arXiv:0710.1954 [hep-ph].
 - [3] G. Weiglein *et al.* [LHC/LC Study Group], Phys. Rept. **426** (2006) 47 [arXiv:hep-ph/0410364].
 - [4] J. F. Gunion, H. E. Haber, G. L. Kane and S. Dawson, “THE HIGGS HUNTER’S GUIDE,” (Addison–Wesley, Reading, 1990).
 - [5] A. Djouadi, arXiv:hep-ph/0503172.
 - [6] A. Djouadi, arXiv:hep-ph/0503173.
 - [7] A. Djouadi, P. M. Zerwas and H. E. Haber, arXiv:hep-ph/9605437.

- [8] A. Djouadi, W. Kilian, M. Muhlleitner and P. M. Zerwas, *Eur. Phys. J. C* **10**, 27 (1999) [arXiv:hep-ph/9903229].
- [9] P. Osland and P. N. Pandita, *Phys. Rev. D* **59**, 055013 (1999) [arXiv:hep-ph/9806351].
F. Boudjema and A. Semenov, *Phys. Rev. D* **66**, 095007 (2002) [arXiv:hep-ph/0201219].
- [10] D. J. Miller and S. Moretti, *Eur. Phys. J. C* **13** (2000) 459 [arXiv:hep-ph/9906395].
- [11] A. Djouadi, W. Kilian, M. Muhlleitner and P. M. Zerwas, *Eur. Phys. J. C* **10** (1999) 45 [arXiv:hep-ph/9904287]. T. Plehn, M. Spira and P. M. Zerwas, *Nucl. Phys. B* **479**, 46 (1996) [Erratum-ibid. *B* **531**, 655 (1998)] [arXiv:hep-ph/9603205]; J. Dai, J. F. Gunion and R. Vega, *Phys. Lett. B* **371**, 71 (1996) [arXiv:hep-ph/9511319] and *Phys. Lett. B* **387**, 801 (1996) [arXiv:hep-ph/9607379]; R. Lafaye, D. J. Miller, M. Muhlleitner and S. Moretti, arXiv:hep-ph/0002238; A. A. Barrientos Bendezu and B. A. Kniehl, *Nucl. Phys. B* **568**, 305 (2000) [arXiv:hep-ph/9908385] and *Phys. Rev. D* **64**, 035006 (2001) [arXiv:hep-ph/0103018]; U. Baur, T. Plehn and D. L. Rainwater, *Phys. Rev. Lett.* **89**, 151801 (2002) [arXiv:hep-ph/0206024], *Phys. Rev. D* **67**, 033003 (2003) [arXiv:hep-ph/0211224], *Phys. Rev. D* **68**, 033001 (2003) [arXiv:hep-ph/0304015], and *Phys. Rev. D* **69**, 053004 (2004) [arXiv:hep-ph/0310056]; *Eur. Phys. J. C* **33**, 41 (2004) [arXiv:hep-ph/0308215]; S. Moretti, *J. Phys. G* **28**, 2567 (2002) [arXiv:hep-ph/0102116]; M. Moretti, S. Moretti, F. Piccinini, R. Pittau and J. Rathsmann, *JHEP* **0712**, 075 (2007) [arXiv:0706.4117 [hep-ph]]; M. Moretti, S. Moretti, F. Piccinini, R. Pittau and A. D. Polosa, *JHEP* **0502**, 024 (2005) [arXiv:hep-ph/0410334].
- [12] M. N. Dubinin and A. V. Semenov, arXiv:hep-ph/9812246.
- [13] M. N. Dubinin and A. V. Semenov, *Eur. Phys. J. C* **28**, 223 (2003) [arXiv:hep-ph/0206205]; P. Osland, P. N. Pandita and L. Selbuz, arXiv:0802.0060 [hep-ph].
- [14] G. Ferrera, J. Guasch, D. Lopez-Val and J. Sola, arXiv:0707.3162 [hep-ph].
- [15] J. F. Gunion and H. E. Haber, *Phys. Rev. D* **67**, 075019 (2003) [arXiv:hep-ph/0207010].
- [16] A. Arhrib and G. Moulhaka, *Nucl. Phys. B* **558**, 3 (1999) [arXiv:hep-ph/9808317].
- [17] A. G. Akeroyd, A. Arhrib and E. Naimi, *Eur. Phys. J. C* **20**, 51 (2001) [arXiv:hep-ph/0002288].
- [18] L. Brucher and R. Santos, *Eur. Phys. J. C* **12** (2000) 87 [arXiv:hep-ph/9907434].
- [19] S. L. Glashow and S. Weinberg, *Phys. Rev. D* **15** (1977) 1958.
- [20] T. P. Cheng and M. Sher, *Phys. Rev. D* **35** (1987) 3484. D. Atwood, L. Reina and A. Soni, *Phys. Rev. D* **55** (1997) 3156; R. Diaz, R. Martinez and J. A. Rodriguez, *Phys. Rev. D* **63**

- (2001) 095007; A. E. Carcamo, R. Martinez and J. A. Rodriguez, Eur. Phys. J. C **50** (2007) 935.
- [21] Thomas J. Weiler, talk given at 8th Vanderbilt Int. Conf. on High Energy Physics, Nashville, Oct 8-10, 1987; Published in Nashville Conf.1987:0219 H. E. Haber, G. L. Kane and T. Sterling, Nucl. Phys. B **161**, 493 (1979).
- [22] A. Denner, R. J. Guth, W. Hollik and J. H. Kuhn, Z. Phys. C **51**, 695 (1991).
- [23] S. Eidelman *et al.* [Particle Data Group], Phys. Lett. B **592** (2004) 1.
- [24] V. D. Barger, J. L. Hewett and R. J. N. Phillips, Phys. Rev. D **41** (1990) 3421.
- [25] A. W. El Kaffas, O. M. Ogreid and P. Osland, arXiv:0709.4203 [hep-ph]. A. Wahab El Kaffas, P. Osland and O. Magne Ogreid, Phys. Rev. D **76**, 095001 (2007) [arXiv:0706.2997 [hep-ph]].
- [26] S. Kanemura, T. Kubota and E. Takasugi, Phys. Lett. B **313**, 155 (1993) [arXiv:hep-ph/9303263].
- [27] A. G. Akeroyd, A. Arhrib and E. M. Naimi, Phys. Lett. B **490**, 119 (2000) [arXiv:hep-ph/0006035]. A. Arhrib, arXiv:hep-ph/0012353. J. Horejsi and M. Kladiva, Eur. Phys. J. C **46**, 81 (2006) [arXiv:hep-ph/0510154].
- [28] M. Sher, Phys. Rept. **179**, 273 (1989). S. Kanemura, T. Kasai and Y. Okada, Phys. Lett. B **471**, 182 (1999) [arXiv:hep-ph/9903289].
- [29] A. Barroso, P. M. Ferreira and R. Santos, arXiv:hep-ph/0507329. P. M. Ferreira, R. Santos and A. Barroso, Phys. Lett. B **603**, 219 (2004) [arXiv:hep-ph/0406231].
- [30] J. Abdallah *et al.* [DELPHI Collaboration], Eur. Phys. J. C **34** (2004) 399; OPAL Phys. Note PN445 (2000); OPAL Phys. Note PN472 (2001).
- [31] G. Abbiendi *et al.* [OPAL Collaboration], Eur. Phys. J. C **40** (2005) 317 [arXiv:hep-ex/0408097].
- [32] J. Abdallah *et al.* [DELPHI Collaboration], Eur. Phys. J. C **38**, 1 (2004) [arXiv:hep-ex/0410017].
- [33] S. Bejar, J. Guasch and J. Sola, Nucl. Phys. B **675** (2003) 270 [arXiv:hep-ph/0307144].
- [34] T. Hahn, Comput. Phys. Commun. **140**, 418 (2001); T. Hahn, C. Schappacher, Comput. Phys. Commun. **143**, 54 (2002); J. Küblbeck, M. Böhm, A. Denner, Comput. Phys. Commun. **60**, 165 (1990).
- [35] T. Hahn and J. I. Illana, arXiv:0708.3652 [hep-ph]. T. Hahn and J. I. Illana, Nucl. Phys. Proc. Suppl. **160** (2006) 101; T. Hahn, M. Perez-Victoria, Comput. Phys. Commun. **118**, 153

- (1999); T. Hahn and J. I. Illana, arXiv:0708.3652 [hep-ph]. T. Hahn, Nucl. Phys. Proc. Suppl. **89**, 231 (2000).
- [36] G. J. van Oldenborgh, Comput. Phys. Commun. **66**, 1 (1991); T. Hahn, Acta Phys. Polon. B **30**, 3469 (1999).
- [37] T. Hahn, Comput. Phys. Commun. **168** (2005) 78 [arXiv:hep-ph/0404043]. T. Hahn, Nucl. Instrum. Meth. A **559** (2006) 273 [arXiv:hep-ph/0509016].
- [38] A. Stange, W. J. Marciano and S. Willenbrock, Phys. Rev. D **49**, 1354 (1994) [arXiv:hep-ph/9309294]; M. A. Diaz and T. J. Weiler, arXiv:hep-ph/9401259. A. Barroso, L. Brucher and R. Santos, Phys. Rev. D **60**, 035005 (1999) [arXiv:hep-ph/9901293]. L. Brucher and R. Santos, Eur. Phys. J. C **12**, 87 (2000) [arXiv:hep-ph/9907434]. A. G. Akeroyd, Nucl. Phys. B **544**, 557 (1999) [arXiv:hep-ph/9806337].
- [39] P. Abreu *et al.* [DELPHI Collaboration], Phys. Lett. B **507**, 89 (2001) [arXiv:hep-ex/0104025].
- [40] A. G. Akeroyd, M. A. Diaz and F. J. Pacheco, Phys. Rev. D **70**, 075002 (2004) [arXiv:hep-ph/0312231].
- [41] I. F. Ginzburg, M. Krawczyk, P. Osland, Nucl. Instrum. Meth. A **472**, 149 (2001).
- [42] A. Arhrib, W. Hollik, S. Penaranda and M. Capdequi Peyranere, Phys. Lett. B **579** (2004) 361.
- [43] S. Kanemura, S. Kiyoura, Y. Okada, E. Senaha and C. P. Yuan, Phys. Lett. B **558** (2003) 157 [arXiv:hep-ph/0211308], S. Kanemura, Y. Okada, E. Senaha and C. P. Yuan, Phys. Rev. D **70** (2004) 115002 [arXiv:hep-ph/0408364].